

Kinetic energy sum spectra in nonmesonic weak decay of hypernuclei

Cesar Barbero^{1,4}, Alfredo P. Galeão², Mahir S. Hussein^{3,5}, and Francisco Krmpotić^{3,4,6}

¹ *Facultad de Ciencias Exactas, Departamento de Física,
Universidad Nacional de La Plata, 1900 La Plata, Argentina*

² *Instituto de Física Teórica, Universidade Estadual Paulista,
Rua Pamplona 145, 01405-900 São Paulo, SP, Brazil*

³ *Departamento de Física Matemática,
Instituto de Física da Universidade de São Paulo,
Caixa Postal 66318, 05315-970 São Paulo, SP, Brazil*

⁴ *Instituto de Física La Plata, CONICET, 1900 La Plata, Argentina*

⁵ *Max-Planck-Institut für Physik komplexer Systeme,
Nöthnitzer Straße 38, D-01187 Dresden, Germany and*

⁶ *Facultad de Ciencias Astronómicas y Geofísicas,
Universidad Nacional de La Plata, 1900 La Plata, Argentina*

(Dated: November 2, 2018)

Abstract

We evaluate the coincidence spectra in the nonmesonic weak decay (NMWD) $\Lambda N \rightarrow nN$ of Λ hypernuclei ${}^4_{\Lambda}\text{He}$, ${}^5_{\Lambda}\text{He}$, ${}^{12}_{\Lambda}\text{C}$, ${}^{16}_{\Lambda}\text{O}$, and ${}^{28}_{\Lambda}\text{Si}$, as a function of the sum of kinetic energies $E_{nN} = E_n + E_N$ for $N = n, p$. The strangeness-changing transition potential is described by the one-meson-exchange model, with commonly used parameterization. Two versions of the Independent-Particle-Shell-Model (IPSM) are employed to account for the nuclear structure of the final residual nuclei. They are: (a) IPSM-a, where no correlation, except for the Pauli principle, is taken into account, and (b) IPSM-b, where the highly excited hole states are considered to be quasi-stationary and are described by Breit-Wigner distributions, whose widths are estimated from the experimental data. All np and nn spectra exhibit a series of peaks in the energy interval $110 \text{ MeV} < E_{nN} < 170 \text{ MeV}$, one for each occupied shell-model state. Within the IPSM-a, and because of the recoil effect, each peak covers an energy interval proportional to A^{-1} , going from $\cong 4 \text{ MeV}$ for ${}^{28}_{\Lambda}\text{Si}$ to $\cong 40 \text{ MeV}$ for ${}^4_{\Lambda}\text{He}$. Such a description could be pretty fair for the light ${}^4_{\Lambda}\text{He}$ and ${}^5_{\Lambda}\text{He}$ hypernuclei. For the remaining, heavier, hypernuclei it is very important, however, to consider as well the spreading in strength of the deep-hole states, and bring into play the IPSM-b approach. Notwithstanding the nuclear model that is employed the results depend only very weakly on the details of the dynamics involved in the decay process proper. We propose that the IPSM is the appropriate lowest-order approximation for the theoretical calculations of the of kinetic energy sum spectra in the NMWD. It is in comparison to this picture that one should appraise the effects of the final state interactions and of the two-nucleon-induced decay mode.

PACS numbers: 21.80.+a, 13.75.Ev, 21.60.Cs, 21.10.Pc

Keywords: nonmesonic hypernuclear decay; energy spectra; strength functions; one meson exchange model

I. INTRODUCTION

Because of the difficulty in detecting neutrons, up to a few years ago only the high energy proton spectra had been measured in the two-body $\Lambda N \rightarrow nN$ nonmesonic weak decay (NMWD) of Λ hypernuclei. The proton-induced transition rates $\Gamma_p \equiv \Gamma(\Lambda p \rightarrow np)$ in ${}^5_\Lambda\text{He}$, ${}^{11}_\Lambda\text{Li}$, and ${}^{12}_\Lambda\text{C}$ have been determined in this way [1, 2, 3]. The corresponding neutron-induced transition rates $\Gamma_n \equiv \Gamma(\Lambda n \rightarrow nn)$ were estimated through the comparison of the measured proton spectrum with that of the intranuclear cascade (INC) calculation where the Γ_n/Γ_p ratio is treated as free parameter. This procedure signalized very large experimental n/p ratios ($\cong 0.9 - 2.0$) [1, 2, 3], in comparison with theoretical estimates ($\cong 0.3 - 0.5$) obtained within the One-Meson-Exchange Potential (OMEP) [4, 5, 6, 7, 8, 9, 10, 11]. (See, for instance, [7, Table 3].). In spite of large uncertainties involved in the indirect evaluation of neutrons, this discrepancy between data and theory was considered to be a serious puzzle in the NMWD.

Yet, quite recently, the above scenario has drastically changed due to the very significant advances in our knowledge (mainly experimental) on both neutron and proton spectra. These advances are:

1. In the experiment E369 were measured high-quality neutron spectra in the decays of ${}^{12}_\Lambda\text{C}$ and ${}^{89}_\Lambda\text{Y}$, which made possible to compare them directly with the corresponding proton spectra, yielding the result $\Gamma_n/\Gamma_p = (0.45 - 0.51) \pm 0.15$ [12].
2. Okada *et al.* [13] have simultaneously measured the energy spectra of neutrons and protons in ${}^5_\Lambda\text{He}$ and ${}^{12}_\Lambda\text{C}$ at a high energy threshold (60 MeV), from where it was inferred that for both hypernuclei $\Gamma_n/\Gamma_p \cong 0.5$.
3. Garbarino, Parreño and Ramos [14, 15, 16] have called attention on the fact that “correlation observables permit a *cleaner* extraction of Γ_n/Γ_p from data than single-nucleon observables”, which has stimulated several experimental searches [17, 18, 19, 20]. They have also done a theoretical evaluation of the pair distributions for: a) the sum of the nN kinetic energies $E = E_n + E_N$, $S_{nN}(E)$, and b) the opening angle θ , $S_{nN}(\cos \theta)$, in the decays of ${}^5_\Lambda\text{He}$ and ${}^{12}_\Lambda\text{C}$. The number of detected nN pairs N_{nN} is proportional to $\Gamma_N = \int S_{nN}(E)dE = \int S_{nN}(\cos \theta)d\cos \theta$, and therefore $N_{nn}/N_{np} \cong \Gamma_n/\Gamma_p$ (see below). The primary weak decay was described by the OMEP dynamics

within the framework of a shell model, while an INC code was used to take into account the strong final state interactions (FSI) involving the primary nucleons and those in the residual nucleus, including the possibility of emission of secondary particles. They conclude that the datum $N_{nn}/N_{np} = 0.44 \pm 0.11$ obtained in KEK-E462 [17] for ${}^5_{\Lambda}\text{He}$ is compatible with an n/p ratio of 0.39 ± 0.11 for this hypernucleus if the two-nucleon induced mode $\Lambda NN \rightarrow nNN$ is neglected, or an even lower value if it is included. Similarly, together with Bauer [21], they found $\Gamma_n/\Gamma_p({}^5_{\Lambda}\text{He}) = 0.46 \pm 0.09$ when the two-nucleon induced mode is neglected and a slightly lower value when it is included. The shell-model used in Refs. [14, 15, 16] is substituted in the last work by a nuclear matter formalism extended to finite nuclei via the local density approximation, while the Monte Carlo INC model is retained to account for the FSI.

4. Quite recently Bauer [22] has given a step forward with his nuclear matter formalism, describing microscopically both the weak decay mechanism and the FSI, confirming in this way that the latter lead to somewhat lower value for the ratio Γ_n/Γ_p in ${}^5_{\Lambda}\text{He}$.
5. Several coincidence emission measurements of the above mentioned spectra have been performed [17, 18, 19, 20, 23, 24], from which were extracted the new experimental results, $\Gamma_n/\Gamma_p({}^5_{\Lambda}\text{He}) = 0.45 \pm 0.11 \pm 0.03$ and $\Gamma_n/\Gamma_p({}^5_{\Lambda}\text{He}) = 0.40 \pm 0.09$, that point towards the solution of the longstanding Γ_n/Γ_p puzzle.¹

Reasoning within the two-body kinematics for the one-nucleon induced NMWD, it is expected that $S_{nN}(E)$ should exhibit a narrow peak at the two-particle energy E close to the decay Q-value, while $S_{nN}(\cos \theta)$ should be restrained within the back-to-back angle $\theta \cong \pi$. Thus, all experimentally observed deviations from such spectral shapes are very frequently attributed to the FSI and/or to the two-nucleon induced processes [17, 18, 19, 20, 23, 24].² However, this is no longer the case when the recoil of the residual nucleus is taken into account, which makes the kinematics to be of a three-body type. Moreover, when the shell model structure is also taken into account the energy spectra will have a bump at each

¹ We note that the relationship $\Gamma_n/\Gamma_p({}^5_{\Lambda}\text{He}) \sim \Gamma_n/\Gamma_p({}^5_{\Lambda}\text{He})$ could have a very simple explanation, similar to that given in Ref. [25] for the asymmetry parameter: $a_{\Lambda}({}^5_{\Lambda}\text{He}) \sim a_{\Lambda}({}^5_{\Lambda}\text{He})$.

² In Refs. [14, 15] it is said that the np energy spectra of the three-body proton-induced decay ${}^5_{\Lambda}\text{He} \rightarrow {}^3\text{H} + n + p$ should exhibit a narrow peak close to its Q-value of 153 MeV, which is only valid when the recoil effect is neglected.

single particle state, the width of which will depend on the magnitude of both the recoil and the spreading in strength of the hole states in the inner shells. Although the detailed structure and fragmentation of hole states are still not well known, the exclusive knockout reactions provide a wealth of information on the structure of single-nucleon states of nuclei. Excitation energies and widths of proton-hole states were systematically measured with quasifree $(p, 2p)$ and $(e, e'p)$ reactions, which revealed the existence of inner orbital shells in nuclei [26, 27, 28, 29, 30, 31, 32, 33, 34].

The aim of the present work is to discuss quantitatively the interplay between the recoil effect and the nuclear shell structure in the kinetic energy sum spectra of NMWD. The paper is organized as follows. In Section II we discuss the calculation of these spectra within the Independent-Particle-Shell-Model (IPSM). In Section III we exhibit the numerical results for $^4_{\Lambda}\text{He}$, $^5_{\Lambda}\text{He}$, $^{12}_{\Lambda}\text{C}$, $^{16}_{\Lambda}\text{O}$, and $^{28}_{\Lambda}\text{Si}$ hypernuclei. In Section IV we discuss these results and their connection with the experimental data. Finally, in Section V, we present several concluding remarks.

II. KINETIC ENERGY SUM SPECTRUM

For the purpose of completeness and clarity, we will first redo the calculation of the decay rate Γ_N using Fermi's golden rule. The novelties here, in comparison with our previous works Refs. [6, 7, 8], are the recoil effect and the spreading of the single-particle configurations. As will be shown in Section IV, their role is of minor importance in the evaluation of the integrated transition rates Γ_N , as well as on the ratio Γ_n/Γ_p , but they are crucial for a correct description of the energy distribution of the transition strength. In fact, a single-particle state $|j_N\rangle$ that is deeply bound in the hypernucleus, after the NMWD can become a highly excited hole-state $|j_N^{-1}\rangle$ in the continuum of the residual nucleus. There it suddenly mixes up with more complicated configurations (2h1p, 3h2p, ... excitations, collective states, *etc.*) spreading its strength in a relatively wide energy interval [35].³ This happens, for instance, with the $1s_{1/2}$ orbital in $^{12}_{\Lambda}\text{C}$, that is separated from the $1p_{3/2}$ state by approximately 23 MeV, which is enough to break the 10 particle system, where the energy of the last excited state amounts to ~ 16.5 MeV.

³ One should keep in mind that the mean life a Λ hyperon is $\tau_\Lambda = 2.63 \times 10^{-10}$ s, while the strong interaction times are of the order of 10^{-21} s.

The NMWD rate of a hypernucleus (in its ground state with spin J_I and energy E_{J_I}) to residual nuclei (in the several allowed states with spins J_F and energies $E_{\alpha_N J_F}$) and two free nucleons nN (with total spin S and total kinetic energy $E_{nN} = E_n + E_N$), reads

$$\begin{aligned}\Gamma_N = & 2\pi \sum_{SM_S \alpha_N J_F M_F} \int |\langle \mathbf{p}_n \mathbf{p}_N S M_S; \alpha_N J_F M_F | V | J_I M_I \rangle|^2 \\ & \times \delta(\Delta_{\alpha_N J_F} - E_r - E_{nN}) \frac{d\mathbf{p}_n}{(2\pi)^3} \frac{d\mathbf{p}_N}{(2\pi)^3}.\end{aligned}\quad (1)$$

Here, V is the hypernuclear nonmesonic weak transition potential, and the wave functions for the kets $|\mathbf{p}_n \mathbf{p}_N S M_S; \alpha_N J_F M_F\rangle$ and $|J_I M_I\rangle$ are assumed to be antisymmetrized and normalized. The label α_N stands for different final states with the same spin J_F , E_r is the recoil energy of the residual nucleus, and

$$\Delta_{\alpha_N J_F} = \Delta + E_{J_I} - E_{\alpha_N J_F}, \quad \text{with} \quad \Delta = M_\Lambda - M = 176 \text{ MeV}, \quad (2)$$

is the liberated energy. The two emitted nucleons are described by plane waves, and initial and final short range correlations are included phenomenologically at a simple Jastrow-like level.

It is convenient to perform a transformation to the relative and c.m. momenta ($\mathbf{p} = \frac{1}{2}(\mathbf{p}_n - \mathbf{p}_N)$, $\mathbf{P} = \mathbf{p}_n + \mathbf{p}_N$), coordinates ($\mathbf{r} = \mathbf{r}_n - \mathbf{r}_N$, $\mathbf{R} = \frac{1}{2}(\mathbf{r}_n + \mathbf{r}_N)$) and orbital angular momenta \mathbf{l} and \mathbf{L} , and to express the energy conservation as

$$E_{nN} + E_r - \Delta_{\alpha_N J_F} = \epsilon_p + \epsilon_P - \Delta_{\alpha_N J_F} = 0, \quad (3)$$

where

$$\epsilon_p = \frac{p^2}{M}, \quad E_r = \frac{P^2}{2M(A-2)}, \quad \epsilon_P = \frac{P^2}{4M} \frac{A}{A-2} = \frac{A}{2} E_r, \quad (4)$$

are, respectively, the energies of the relative motion of the outgoing pair, of the recoil, and of the total c.m. motion (including the recoil). Following step by step the analytical developments done in Ref. [6], the transition rate can be expressed as

$$\Gamma_N = \int_0^\Delta \frac{d\Gamma_N}{d\epsilon_P} d\epsilon_P \quad (5)$$

where we have defined (see [6, Eqs. (2.13) and (2.14)])

$$\begin{aligned}\frac{d\Gamma_N}{d\epsilon_P} = & \frac{16M^3}{\pi} \left(\frac{A-2}{A} \right)^{3/2} \hat{J}_I^{-2} \sum_{S \lambda l L T J \alpha_N J_F} \sqrt{\epsilon_P(\Delta_{\alpha_N J_F} - \epsilon_P)} \\ & \times \left| \sum_{j_N} \mathcal{M}(pPLL\lambda SJT; j_N) \langle J_I | \left(a_{j_N}^\dagger a_{j_\Lambda}^\dagger \right)_J | \alpha_N J_F \rangle \right|^2,\end{aligned}\quad (6)$$

it being understood that the square root is to be replaced by zero whenever its argument is negative. The angular momentum couplings $\mathbf{l} + \mathbf{L} = \boldsymbol{\lambda}$ and $\boldsymbol{\lambda} + \mathbf{S} = \mathbf{J}$ have been carried out, $\hat{J} \equiv \sqrt{2J+1}$, and $A = Z + N + 1$ is the total number of baryons.

It is self-evident that for $A \rightarrow \infty$ one obtains the same result as in Refs. [6, 7, 8]. It is also worth noting that the overall outcome of the recoil on Γ_N is very small, mostly because the effect of the factor $\left(\frac{A-2}{A}\right)^{3/2}$ in Eq. (6) is, to a great extent, cancelled by the effect of the factor $\left(\frac{A}{A-2}\right)^{3/2}$ originating from $\sqrt{\epsilon_P(\Delta_{\alpha_N J_F} - \epsilon_P)}d\epsilon_P$. This is the reason why we have not included the recoil previously.

The spectrum of Γ_N as a function of E_{nN} is now easily obtained from Eq. (6) by means of the relation

$$E_{nN} = \Delta_{\alpha_N J_F} - \frac{2}{A}\epsilon_P, \quad (7)$$

as follows from (3) and (4). Calling $E \equiv E_{nN}$, one gets

$$\Gamma_N = \int_0^\Delta S_{nN}(E) dE \quad (8)$$

with

$$\begin{aligned} S_{nN}(E) &= \frac{4M^3}{\pi} \sqrt{A(A-2)^3} \hat{J}_I^{-2} \sum_{S\lambda lLTJ\alpha_N J_F} \sqrt{(\Delta_{\alpha_N J_F} - E)(E - \Delta'_{\alpha_N J_F})} \\ &\times \left| \sum_{j_N} \mathcal{M}(pPlL\lambda SJT; j_N) \langle J_I | \left(a_{j_N}^\dagger a_{j_\Lambda}^\dagger \right)_J | \alpha_N J_F \rangle \right|^2, \end{aligned} \quad (9)$$

where

$$\begin{aligned} p &= \sqrt{\frac{MA}{2} (E - \Delta'_{\alpha_N J_F})}, \\ P &= \sqrt{2M(A-2)(\Delta_{\alpha_N J_F} - E)}, \end{aligned} \quad (10)$$

$$\Delta'_{\alpha_N J_F} = \Delta_{\alpha_N J_F} \frac{A-2}{A}, \quad (11)$$

and the condition

$$\Delta'_{\alpha_N J_F} \leq E \leq \Delta_{\alpha_N J_F}, \quad (12)$$

has to be fulfilled for each contribution.

As previously [6, 7, 8], it will be assumed that the hyperon in the state j_Λ , with single-particle energy ϵ_{j_Λ} , is weakly coupled to the $A-1$ core, with spin J_C and energy $E_C =$

$E_{J_I} - \epsilon_{j_\Lambda}$. Then the initial state is $|J_I\rangle \equiv |(J_C j_\Lambda) J_I\rangle$, and the spectroscopic amplitude $\langle J_I| \left(a_{j_N}^\dagger a_{j_\Lambda}^\dagger \right)_J | \alpha_N J_F \rangle$ can be rewritten as

$$\langle J_I| \left(a_{j_N}^\dagger a_{j_\Lambda}^\dagger \right)_J | \alpha_N J_F \rangle = (-)^{J_F + J + J_I} \hat{J} \hat{J}_I \left\{ \begin{array}{ccc} J_C & J_I & j_\Lambda \\ J & j_N & J_F \end{array} \right\} \langle J_C | a_{j_N}^\dagger | \alpha_N J_F \rangle. \quad (13)$$

The following two approaches for the final states $|\alpha_N J_F\rangle$ will be examined within the IPSM.

A. IPSM-a

Here, we completely ignore the residual interaction and, consequently, the only states $|\alpha_N J_F\rangle$ giving a nonzero result in Eq. (13) and therefore contributing to Eq. (9) are those obtained by the weak coupling, and properly antisymmetrizing, of the one hole (1h) states $|j_N^{-1}\rangle$ to the core ground-state $|J_C\rangle$. That is, recalling that we completely ignore the residual interaction in this approximation,

$$|\alpha_N J_F\rangle \mapsto |j_N J_F\rangle \equiv |(J_C, j_N^{-1}) J_F\rangle, \quad \text{and} \quad E_{\alpha_N J_F} \mapsto E_{j_N} \equiv E_C - \epsilon_{j_N}, \quad (14)$$

where ϵ_{j_N} is the single-particle energy of state j_N . As an illustration, in the case of $^{28}_\Lambda\text{Si}$ the model space contains four single-particle states, both for protons and for neutrons ($n_p = n_n = 4$), namely, $1s_{1/2}$, $1p_{3/2}$, $1p_{1/2}$ and $1d_{5/2}$. Thus, for $|J_C\rangle = |1d_{5/2}n^{-1}\rangle$, the final states (14) are constructed by adding two holes in the ^{28}Si nucleus, and read:

$$\begin{array}{ll} \underline{^{28}_\Lambda\text{Si} \rightarrow nn + ^{26}\text{Si}} & \underline{^{28}_\Lambda\text{Si} \rightarrow np + ^{26}\text{Al}} \\ \\ |(1d_{5/2}n^{-1})^2; 0, 2, 4\rangle & |(1d_{5/2}n^{-1}1d_{5/2}p^{-1}); 0, 1, 2, 3, 4, 5\rangle \\ |1d_{5/2}n^{-1}1s_{1/2}n^{-1}; 2, 3\rangle & |1d_{5/2}n^{-1}1s_{1/2}p^{-1}; 2, 3\rangle \\ |1d_{5/2}n^{-1}1p_{1/2}n^{-1}; 2, 3\rangle & |1d_{5/2}n^{-1}1p_{1/2}p^{-1}; 2, 3\rangle \\ |1d_{5/2}n^{-1}1p_{3/2}n^{-1}; 1, 2, 3, 4\rangle & |1d_{5/2}n^{-1}1p_{3/2}p^{-1}; 1, 2, 3, 4\rangle. \end{array} \quad (15)$$

The summation on J_F in (9) can be performed for each single-particle state j_N , as done in [7, Eqs. (11), (12), (13)]. One gets

$$S_{nN}(E) = \frac{4M^3}{\pi} \sqrt{A(A-2)^3} \sum_{j_N} \sqrt{(\Delta_{j_N} - E)(E - \Delta'_{j_N})} \mathcal{F}_{j_N}(pP), \quad (16)$$

where

$$\mathcal{F}_{j_N}(pP) = \sum_{J=|j_N-1/2|}^{J=j_N+1/2} F_{j_N}^J \sum_{SIL\lambda T} \mathcal{M}^2(pPlL\lambda SJT; j_N), \quad (17)$$

with the spectroscopic factors $F_{j_N}^J$ exhibited in [7, Table 1]. The maximum and minimum liberated energies are, respectively,

$$\Delta_{\alpha_N J_F} \mapsto \Delta_{j_N} = \Delta + \epsilon_{j_N} + \epsilon_{j_N} \quad (18)$$

and

$$\Delta'_{j_N} = \Delta_{j_N} \frac{A-2}{A}, \quad (19)$$

and the momenta are given by

$$p = \sqrt{\frac{MA}{2} (E - \Delta'_{j_N})} \quad \text{and} \quad P = \sqrt{2M(A-2)(\Delta_{j_N} - E)}. \quad (20)$$

B. IPSM-b

Formally, one starts from the unperturbed basis $|i_N J_F\rangle_0$ with $i_N = 1, 2, \dots, n_N, n_N + 1, \dots$, where for $i_N \leq n_N$ we have the same simple doorway states $|j_N J_F\rangle$ in Eq. (14) (listed in Eq. (15) for ^{28}Si), while for $i_N \geq n_N + 1$ we have more complicated bound configurations (such as $3h1p, 4h2p, \dots$ in the case of ^{28}Si) as well as those including unbound single-particle states in the continuum. As in Ref. [35], the perturbed eigenkets $|\alpha_N J_F\rangle$ and eigenvalues $E_{\alpha_N J_F}$ are obtained by diagonalizing the matrix ${}_0\langle i_N J_F | H | i'_N J_F \rangle_0$ of the exact Hamiltonian H :

$$\langle \alpha_N J_F | H | \alpha'_N J_F \rangle = E_{\alpha_N J_F} \delta_{\alpha_N \alpha'_N} \quad (21)$$

with

$$\begin{aligned} |\alpha_N J_F\rangle &= \sum_{i_N=1}^{\infty} C_{i_N}^{\alpha_N J_F} |i_N J_F\rangle_0 \\ &= \sum_{j_N} C_{j_N}^{\alpha_N J_F} |j_N J_F\rangle + \sum_{i_N=n_N+1}^{\infty} C_{i_N}^{\alpha_N J_F} |i_N J_F\rangle_0. \end{aligned} \quad (22)$$

It is easy to see that only the ket $|j_N J_F\rangle$ in the expansion (22) will contribute to the matrix element $\langle J_C | |a_{j_N}^\dagger| |\alpha_N J_F\rangle$ in Eq. (13). Therefore Eq. (9) takes the form

$$\begin{aligned} S_{nN}(E) &= \frac{4M^3}{\pi} \sqrt{A(A-2)^3} \\ &\times \sum_{j_N \alpha_N J_F} |C_{j_N}^{\alpha_N J_F}|^2 \sqrt{(\Delta_{\alpha_N J_F} - E)(E - \Delta'_{\alpha_N J_F})} \mathcal{F}(p, P; j_N J_F), \end{aligned} \quad (23)$$

where

$$\mathcal{F}(p, P; j_N J_F) = \hat{J}_I^{-2} \sum_{lL\lambda SJT} \left| \mathcal{M}(pPlL\lambda SJT; j_N) \langle J_I | \left(a_{j_N}^\dagger a_{j_\Lambda}^\dagger \right)_J | j_N J_F \rangle \right|^2. \quad (24)$$

To evaluate the amplitudes $C_{j_N}^{\alpha_N J_F}$ one would have to choose the appropriate Hamiltonian H and the unperturbed basis $|i_N J_F\rangle_0$, and solve the eigenvalue problem (21). We will not do this here. Instead, we will make a phenomenological estimate. First, because of the high density of states, we will convert the discrete energies $\Delta_{\alpha_N J_F}$ into the continuous variable ε , and the discrete sum on α_N into an integral on ε , *i.e.*,

$$\Delta_{\alpha_N J_F} \rightarrow \varepsilon, \quad \sum_{\alpha_N J_F} |C_{j_N}^{\alpha_N J_F}|^2 \rightarrow \sum_{J_F} \int_{-\infty}^{\infty} |C_{j_N J_F}(\varepsilon)|^2 \rho_{J_F}(\varepsilon) d\varepsilon, \quad (25)$$

where $\rho_{J_F}(\varepsilon)$ is the density of perturbed states with angular momentum J_F . In this way the spectrum (23) becomes

$$\begin{aligned} S_{nN}(E) &= \frac{4M^3}{\pi} \sqrt{A(A-2)^3} \\ &\times \sum_{j_N J_F} \int_{-\infty}^{\infty} P_{j_N J_F}(\varepsilon) \sqrt{(\varepsilon - E)(E - \varepsilon')} \mathcal{F}(p, P; j_N J_F) d\varepsilon, \end{aligned} \quad (26)$$

where

$$P_{j_N J_F}(\varepsilon) = |C_{j_N J_F}(\varepsilon)|^2 \rho_{J_F}(\varepsilon) \quad (27)$$

is called the *strength function* [35, 36, 37] and represents the probability of finding the configuration $|j_N J_F\rangle \equiv |(J_C, j_N^{-1}) J_F\rangle$ per unit energy interval. Moreover,

$$\begin{aligned} p &= \sqrt{\frac{MA}{2}(E - \varepsilon')}, \\ P &= \sqrt{2M(A-2)(\varepsilon - E)}, \end{aligned} \quad (28)$$

$$\varepsilon' = \varepsilon \frac{A-2}{A}, \quad (29)$$

and the condition

$$\varepsilon' \leq E \leq \varepsilon, \quad (30)$$

has to be fulfilled throughout the ε integration. It is convenient to introduce the averaged strength function

$$P_{j_N}(\varepsilon) = \frac{1}{\dim(j_N J_C)} \sum_{J_F=|J_C-j_N|}^{J_C+j_N} P_{j_N J_F}(\varepsilon), \quad (31)$$

where

$$\dim(j_N J_C) = \begin{cases} 2j_N + 1 & \text{for } j_N \leq J_C, \\ 2J_C + 1 & \text{for } J_C < j_N. \end{cases} \quad (32)$$

This allows to simplify Eq. (26) by making the approximation $P_{j_N J_F}(\varepsilon) \approx P_{j_N}(\varepsilon)$ to get

$$\begin{aligned} S_{nN}(E) &= \frac{4M^3}{\pi} \sqrt{A(A-2)^3} \\ &\times \sum_{j_N} \int_{-\infty}^{\infty} P_{j_N}(\varepsilon) \sqrt{(\varepsilon - E)(E - \varepsilon')} \mathcal{F}_{j_N}(pP) d\varepsilon, \end{aligned} \quad (33)$$

where we noticed that the summation of $\mathcal{F}(p, P; j_N J_F)$ over J_F gives the function defined in Eq. (17).

The IPSM-a results would be recovered if one made the further approximation

$$P_{j_N}(\varepsilon) = \delta(\varepsilon - \Delta_{j_N}). \quad (34)$$

Here, in IPSM-b, the δ -functions (34) will be used for the strictly stationary states, while for the fragmented hole states we will use Breit-Wigner distributions,

$$P_{j_N}(\varepsilon) = \frac{2\gamma_{j_N}}{\pi} \frac{1}{\gamma_{j_N}^2 + 4(\varepsilon - \Delta_{j_N})^2}, \quad \int_{-\infty}^{\infty} P_{j_N}(\varepsilon) d\varepsilon = 1, \quad (35)$$

where γ_{j_N} are the widths of the resonance centroids at energies Δ_{j_N} (see [35, Eq.(2.11.22)]).

It might be important to point out that, since both strength functions $P_{j_N}(\varepsilon)$ are normalized to unit, their effect on integrated observables like the decay rates Γ_N is expected to be small even if they considerably affect the spectra. This will be further investigated in Section IV.

III. NUMERICAL RESULTS

In Figs. 1 and 2 we show, respectively, the normalized energy spectra $S_{np}(E)/\Gamma_p$ and $S_{nn}(E)/\Gamma_n$ for ${}^4_{\Lambda}\text{He}$, ${}^5_{\Lambda}\text{He}$, ${}^{12}_{\Lambda}\text{C}$, ${}^{16}_{\Lambda}\text{O}$, and ${}^{28}_{\Lambda}\text{Si}$ hypernuclei, evaluated within the full OMEP, that comprises the $(\pi, \eta, K, \rho, \omega, K^*)$ mesons. The single-particle energies for the strictly stationary hole states have been taken from Wapstra and Gove's compilation [38], and those of the quasi-stationary ones have been estimated from the studies of the quasi-free scattering processes $(p, 2p)$ and $(e, e'p)$ [26, 27, 28, 29, 30, 31, 32, 33, 34].

The two IPSM approaches exhibit some quite important differences:

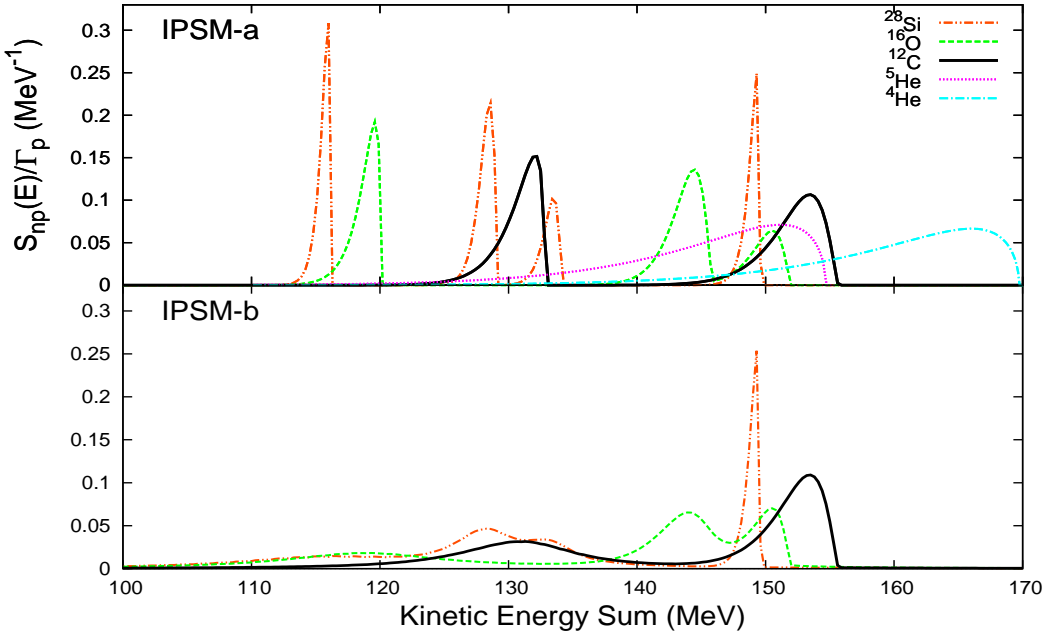


FIG. 1: (Color online) Normalized energy spectra $S_{np}(E)/\Gamma_p$ for ${}^4_\Lambda\text{He}$, ${}^5_\Lambda\text{He}$, ${}^{12}\text{C}$, ${}^{16}\text{O}$, and ${}^{28}\text{Si}$ hypernuclei for the full OMEP obtained within the approaches IPSM-a (upper panel) and IPSM-b (lower panel). For the s -shell hypernuclei, only the IPSM-a approach has been used.

a) *IPSM-a*: The spectra cover the energy region $110 \text{ MeV} < E < 170 \text{ MeV}$ and contain one or more peaks, the number of which is equal to the number of shell-model orbitals $1s_{1/2}, 1p_{3/2}, 1p_{1/2}, 1d_{5/2}, 2s_{1/2}, 1d_{3/2} \dots$ that are either fully or partly occupied in $|J_C\rangle$. Before including the recoil, all these peaks would be just spikes at the liberated energies Δ_{j_N} , as can be seen from (3) setting $E_r = 0$. With the recoil effect, they behave as

$$S_{nN}(E \cong \Delta_{j_N}) \sim \sqrt{(\Delta_{j_N} - E)(E - \Delta'_{j_N})} e^{-M(A-2)(\Delta_{j_N} - E)b^2}, \quad (36)$$

and develop rather narrow widths $\sim [b^2 M(A-2)]^{-1}$, where b is the harmonic oscillator size parameter, which has been taken from Ref. [5]. These widths go from $\cong 3 \text{ MeV}$ for ${}^{28}\text{Si}$ to $\cong 20 \text{ MeV}$ for ${}^4_\Lambda\text{He}$, as indicated in the upper panels of the just mentioned figures.

b) *IPSM-b*: In the lower panels of the same figures are shown the results obtained when the recoil is convoluted with the Breit-Wigner distributions (35) for the strength functions of the fragmented deep hole states. The widths γ_{j_N} have been estimated from

Refs. [26, 27, 28, 29, 30, 31, 32, 33, 34, 35], and in particular from [26, Figure 11] and [30, Table 1], with the results: $\gamma_{1s_{1/2}} = 9$ MeV in $^{12}\Lambda\text{C}$, $\gamma_{1s_{1/2}} = 14$ MeV and $\gamma_{1p_{3/2}} = 3$ MeV in $^{16}\Lambda\text{O}$ ⁴, and $\gamma_{1s_{1/2}} = 16$ MeV and $\gamma_{1p_{3/2}} = \gamma_{1p_{1/2}} = 5$ MeV in $^{28}\Lambda\text{Si}$, both for protons and neutrons. One sees that, except for the ground states, the narrow peaks engendered by the recoil effect become now pretty wide bumps.

We feel that the above rather rudimentary parameterization could be realistic enough for a qualitative discussion of the kinetic energy sum spectra. A more accurate model should be probably necessary for a full quantitative study and comparison with data.

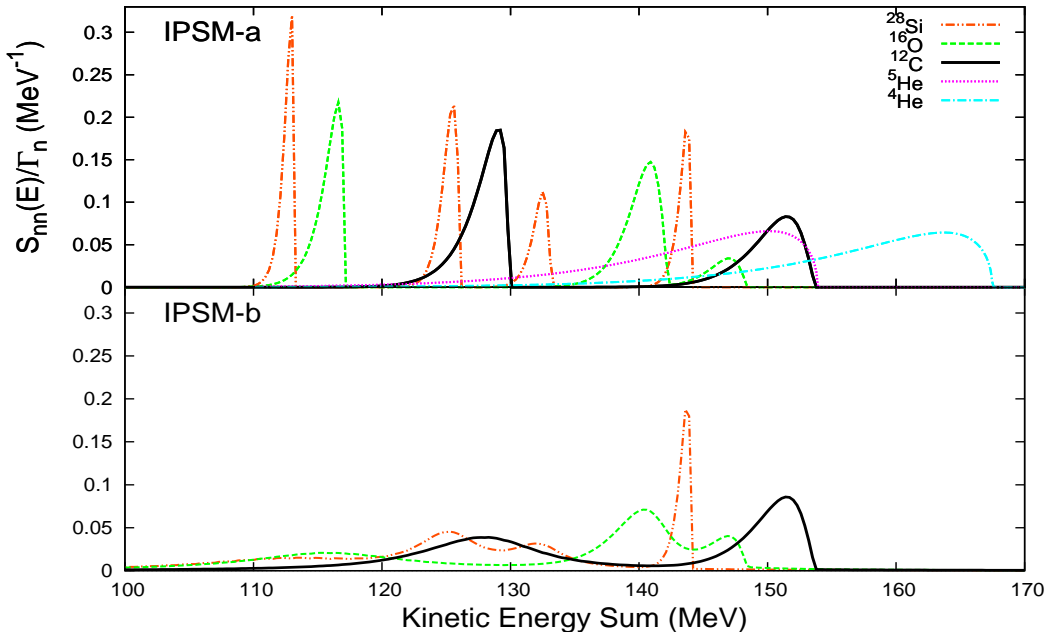


FIG. 2: (Color online) Normalized energy spectra $S_{nn}(E)/\Gamma_n$ for $^4\Lambda\text{He}$, $^5\Lambda\text{He}$, $^{12}\Lambda\text{C}$, $^{16}\Lambda\text{O}$, and $^{28}\Lambda\text{Si}$ hypernuclei for the full OMEP, obtained within the approaches IPSM-a (upper panel) and IPSM-b (lower panel). For the s -shell hypernuclei, only the IPSM-a approach has been used.

⁴ The $3/2^-_1$ peak is at 6.32 MeV, but small amounts of the $p_{3/2}$ strength are also fragmented to the states of 9.93 MeV and 10.7 MeV [34].

IV. GENERAL CONSIDERATIONS AND CONNECTION WITH DATA

The normalized spectra shown in Figs. 1 and 2 have a very weak dependence on the dynamics involved in the NMWD process proper, and almost identical shapes would have been obtained if only the One-Pion Exchange Potential (OPEP) had been taken into account. To understand this fact one can appeal to the s-wave approximation, which assumes that only the relative matrix elements of the form $\langle p, lSJT|V|0JJT \rangle$, *i.e.*, with the ΛN system in an s-state, significantly contribute to $\mathcal{M}(pPlL\lambda SJT; j_N)$. This has been examined quantitatively, for p -shell hypernuclei, in Ref. [39]; see also the Refs. [5, 6]. Furthermore, as we have discussed in Ref. [25], those matrix elements depend only very weakly on the relative momentum p and, as such, they can be evaluated at the maximum value of $p = p_\Delta = \sqrt{M\Delta}$, which corresponds to $P = 0$ or, according to Eq. (20), to $E = \Delta_{j_N} \cong \Delta$. Thus the energy dependence of $S_{nN}(E)/\Gamma_N$ remains exclusively in kinematical phase-space factors, and the position and width of the peaks will be unaffected by the dynamics of the decay process, which will influence, to some extent, only their relative heights. This is illustrated in the case of the np spectrum for $^{12}_\Lambda C$ in Fig. 3, showing that even this latter effect is very small. The comparison between the normalized spectra obtained with the full OMEP and with the $\pi + K$ exchange potential would give an almost perfect superposition.

Needless to stress that the transition probabilities Γ_N do strongly depend on the hypernuclear transition potential, but this dependence is washed out in the ratios defining the normalized spectra. Conversely, for a given choice of transition potential both shell model approaches discussed here yield very similar results for the Γ_N . These points are illustrated in Table I, where one can also see that, as already anticipated in Section II, the effect of the recoil on these quantities is negligible.

One can then summarize our findings by saying that in light systems ($^4_\Lambda He$ and $^5_\Lambda He$) the kinetic energy sum coincidence spectra $S_{nN}(E)$, normalized to the total decay rates Γ_N , basically depend on energies associated with the three-body kinematics. The differences between $S_{np}(E)$ and $S_{nn}(E)$ are mainly due to the differences in the proton and neutron separation energies and in the spectroscopic factors $F_{j_N}^J$. For the remaining hypernuclei it is imperative, in addition, to take into account that most of the hole states are fragmented and consequently one has to consider the spreading of their strengths.

The residual interaction among the valence particles and their coupling to the collective

TABLE I: Nonmesonic decay rates in units of $\Gamma_\Lambda^0 = 2.50 \times 10^{-6}$ eV and n/p branching ratios for ${}_{\Lambda}^{12}\text{C}$, ${}_{\Lambda}^{16}\text{O}$ and ${}_{\Lambda}^{28}\text{Si}$ computed with several transition potentials and using the IPSM-a and IPSM-b approaches. The values obtained in the IPSM-a framework but neglecting the recoil are shown within parentheses.

	Γ_n	Γ_p	Γ_n/Γ_p
${}_{\Lambda}^{12}\text{C}$			
IPSM-a			
OMEP	0.249 (0.249)	0.956 (0.960)	0.260 (0.259)
$\pi + K$	0.244 (0.244)	0.755 (0.758)	0.323 (0.322)
IPSM-b			
OMEP	0.246	0.947	0.260
$\pi + K$	0.241	0.748	0.322
OPEP	0.142	1.004	0.141
${}_{\Lambda}^{16}\text{O}$			
IPSM-a			
OMEP	0.290 (0.290)	1.024 (1.027)	0.283 (0.282)
$\pi + K$	0.287 (0.287)	0.811 (0.813)	0.354 (0.353)
IPSM-b			
OMEP	0.285	1.009	0.282
$\pi + K$	0.282	0.799	0.353
${}_{\Lambda}^{28}\text{Si}$			
IPSM-a			
OMEP	0.348 (0.348)	1.163 (1.164)	0.299 (0.299)
$\pi + K$	0.341 (0.341)	0.934 (0.935)	0.365 (0.365)
IPSM-b			
OMEP	0.345	1.123	0.307
$\pi + K$	0.338	0.903	0.374

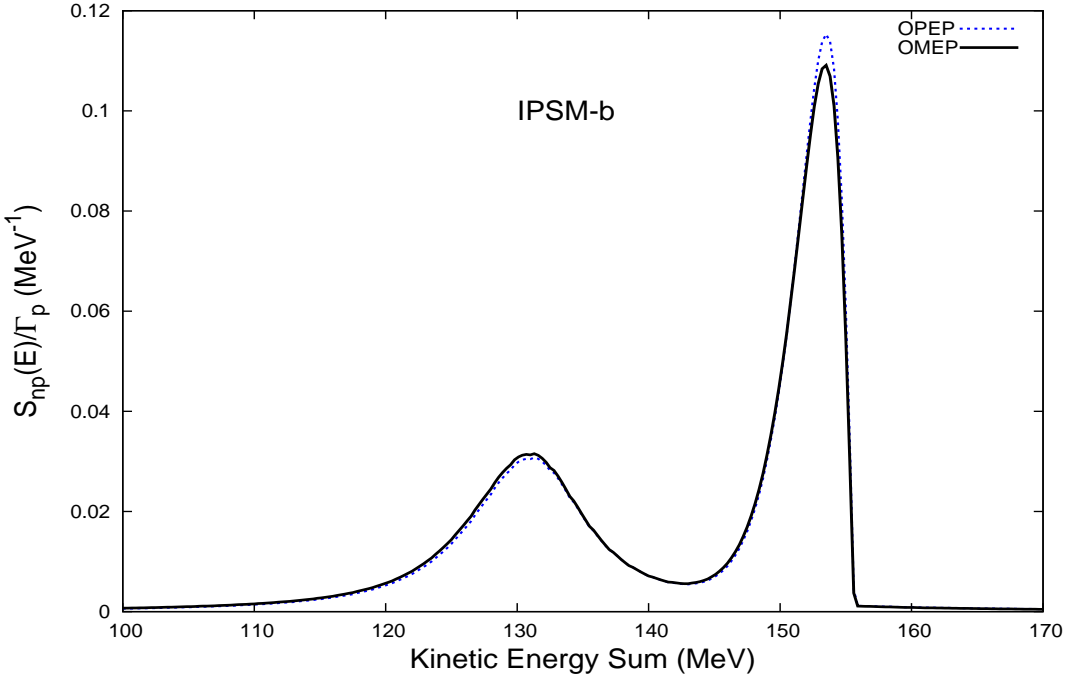


FIG. 3: (Color online) Normalized energy spectra $S_{np}(E)/\Gamma_p$ for the decay of $^{12}\Lambda C$, computed with the full OMEP and the OPEP in the framework of the IPSM-b.

rotational and/or vibrational motions are not explicitly considered in the present work. But it is not expected that these would modify qualitatively the above scenario. It might be worth noting, nevertheless, that the pairing force would be capable of shifting some of the strength from the occupied levels to higher lying orbitals. For instance, in $^{12}\Lambda C$ a part of the $1p_{3/2}$ strength would be moved up into the $1p_{1/2}$ orbital, while in $^{28}\Lambda Si$ the strength would be moved from the $1d_{5/2}$ level into the empty $2s_{1/2}$ and $1d_{3/2}$ states. However, we believe that the coupling of the deep-hole states to other more complicated configurations through the residual interaction, which is treated here in a phenomenological way, is by far a more relevant effect for the physics discussed in the present paper.

We would not like end this paper without making some comments on the relation between the formalism developed here and the experiments. To this end we shall follow closely the discussion in Ref. [40]. The theoretical prediction for the number of nN pairs detected in coincidence with kinetic energy sum E within the interval dE can be written as

$$dN_{nN}(E) = C_{nN}(E)S_{nN}(E)dE, \quad (37)$$

where the factor $C_{nN}(E)$ depends on the experimental environment and includes all quanti-

ties and effects not considered in $S_{nN}(E)$, such as the number of produced hypernuclei, the detection efficiency and acceptance, *etc.* Assuming, for simplicity, that the experimental spectra have already been corrected for detection efficiency and acceptance and that the possible remaining energy dependence in this factor can be neglected, the predicted total number of detected events N_{nN} can be related to Γ_N as follows:

$$N_{nN} = \int \frac{dN_{nN}(E)}{dE} dE = C_{nN} \int S_{nN}(E) dE = C_{nN} \Gamma_N. \quad (38)$$

This allows us to rewrite (37) in the form

$$\frac{dN_{nN}(E)}{dE} = N_{nN} \frac{S_{nN}(E)}{\Gamma_N}. \quad (39)$$

What is measured in an experiment is the number of pairs $\Delta N_{nN}^{exp}(E_i)$ at a given energy E_i within a fixed energy bin ΔE_{nN} , *i.e.*, $\Delta N_{nN}^{exp}(E_i)/\Delta E_{nN}$. The total number of observed events is

$$N_{nN}^{exp} = \sum_{i=1}^m \Delta N_{nN}^{exp}(E_i), \quad (40)$$

where m is the number of bins. The spectrum $S_{nN}(E)$ can be normalized to the experimental one by identifying N_{nN} in (39) with N_{nN}^{exp} . Thus, the quantity that we have to confront with measurements is

$$\Delta N_{nN}(E) = N_{nN}^{exp} \Delta E_{nN} \frac{S_N(E)}{\Gamma_N}. \quad (41)$$

For instance, to compare the experimental data given in [23, Fig.11] with our calculations shown in Figs. 1 and 2, the latter should be multiplied by the factors $N_{np}^{exp} \cdot \Delta E_{np} = 87 \times 5$ MeV = 435 MeV, and $N_{nn}^{exp} \cdot \Delta E_{nn} = 19 \times 5$ MeV = 95 MeV, respectively.

Here we have, neither considered the resolution of the detector system, nor explicitly included the FSI. Also, we have ignored the three-body ΛNN decay contributions. As a consequence it is very reasonable that only a wide bump at about 140 MeV would appear in the experimental spectra for $^{12}\Lambda$ C and heavier hypernuclei. The IPSM predicts quite similar spectra for the np and nn pairs. Moreover, from the present results one could venture to say that the neutron bump should lie at a smaller energy than the proton one. This agrees only marginally with the experiments performed so far, where important differences between the np and nn spectra have been observed.

V. CONCLUDING REMARKS

In this paper, we have investigated, in the framework of the independent particle shell model (IPSM), the effects of the recoil of the residual nucleus and of the spreading in strength of the deep-hole states on nonmesonic weak decay (NMWD) observables. We conclude that, while their effect is of minor importance for integrated observables like the decay rates and the n/p branching ratio, they play a crucial role in determining the shapes of the normalized kinetic energy sum coincidence spectra of nn and np pairs. For the spectra of s -shell hypernuclei, the recoil effect is the most important one.

In summary, we believe that the IPSM is the appropriate lowest-order approximation for the theoretical calculation of the two-particle spectra in the NMWD when: 1) the recoil effect is included, and 2) the fragmentation of the strengths of the deep-hole states is taken into account. It is in comparison to this picture that one should appraise the effects of the FSI and of the two-nucleon-induced decay mode.

The consequences of the two effects dealt with here on the one-particle kinetic energy spectra and on the opening angle distributions of np and nn pairs will be discussed elsewhere.

Acknowledgments

This work was partly supported by the Brazilian agencies CNPq and FAPESP, and by the Argentinian agency CONICET under contract PIP 6159. M. S. Hussein thanks the Martin Gutzwiller program at the Max Planck Institute for the Physics of Complex Systems-Dresden for support.

- [1] J. J. Szymanski, P. D. Barnes, G. E. Diebold, R. A. Eisenstein, G. B. Franklin, R. Grace, D. W. Hertzog, C. J. Maher, B. P. Quinn, R. Rieder, J. Seydoux, W. R. Wharton, S. Bart, R. E. Chrien, P. Pile, R. Sutter, Y. Xu, R. Hackenburg, E. V. Hungerford, T. Kishimoto, L. G. Tang, B. Bassalleck, and R. L. Stearns, Phys. Rev. **C43**, 849 (1991).
- [2] H. Noumi, S. Ajimura, H. Ejiri, A. Higashi, T. Kishimoto, D. R. Gill, L. Lee, A. Olin, T. Fukuda, and O. Hashimoto, Phys. Rev. **C52**, 2936 (1995).

- [3] O. Hashimoto, S. Ajimura, K. Aoki, H. Bhang, T. Hasegawa, H. Hotchi, Y. D. Kim, T. Kishimoto, K. Maeda, H. Noumi, Y. Ohta, K. Omata, H. Outa, H. Park, Y. Sato, M. Sekimoto, T. Shibata, T. Takahashi, and M. Youn, Phys. Rev. Lett. **88**, 042503 (2002).
- [4] A. Parreño and A. Ramos, Phys. Rev. **C 65**, 015204 (2001).
- [5] K. Itonaga, T. Ueda, and T. Motoba, Phys. Rev. **C 65**, 034617 (2002).
- [6] C. Barbero, D. Horvat, F. Krmpotić, T. T. S. Kuo, Z. Narančić, and D. Tadić, Phys. Rev. **C 66**, 055209 (2002).
- [7] F. Krmpotić and D. Tadić, Braz. J. Phys. **33**, 187 (2003).
- [8] C. Barbero, C. De Conti, A. P. Galeão, and F. Krmpotić, Nucl. Phys. **A726**, 267 (2003).
- [9] E. Bauer and F. Krmpotić, Nucl. Phys. **A 717**, 217 (2003); **A 739**, 109 (2004).
- [10] C. Barbero, A. P. Galeão, and F. Krmpotić, Phys. Rev. **C 72**, 035210 (2005).
- [11] G. Garbarino, arXiv:nucl-th/0701049.
- [12] J.H. Kim *et al.*, Phys. Rev. **C 68**, 065201 (2003).
- [13] S. Okada *et al.*, Phys. Lett. **B597**, 249 (2004).
- [14] G. Garbarino, A. Parreño, and A. Ramos, Phys. Rev. Lett. **91**, 112501 (2003).
- [15] G. Garbarino, A. Parreño, and A. Ramos, Phys. Rev. **C 69**, 054603 (2004).
- [16] G. Garbarino, A. Parreño, and A. Ramos, Nucl. Phys. **A754**, 137c (2005).
- [17] H. Outa *et al.*, Nucl. Phys. **A754**, 157c (2005).
- [18] S. Okada *et al.*, Nucl. Phys. **A752**, 169c (2005).
- [19] B.H. Kang *et al.*, Phys. Rev. Lett. **96**, 062301 (2006).
- [20] M.J. Kim *et al.*, Phys. Lett. **B641**, 28 (2006).
- [21] E. Bauer, G. Garbarino, A. Parreño, and A. Ramos, arXiv:nucl-th/0602066.
- [22] E. Bauer, Nucl.Phys. **A781**, 424 (2007); **A796**, 11 (2007).
- [23] J.D. Parker *et al.*, Phys. Rev. **C 76**, 035501 (2007).
- [24] H. Bhang *et al.*, Eur. Phys. J. **A33**, 259 (2007).
- [25] C. Barbero, A. P. Galeão, and F. Krmpotić, Phys. Rev. **C 76**, 054321 (2007).
- [26] G. Jacob and T. A. J. Maris, Rev. Mod. Phys. **45**, 6 (1973).
- [27] S. Frullani, J. Mougey, Adv. Nucl. Phys. **14**, 1 (1984).
- [28] S.L. Belostotskii *et al.*, Sov. J. Nucl. Phys. **41**, 903 (1985); S.S. Volkov *et al.*, Sov. J. Nucl. Phys. **52**, 848 (1990).
- [29] M. Leuschner *et al.*, Phys. Rev. **C 49**, 955 (1994).

- [30] T. Yamada, M. Takahashi, and K. Ikeda, Phys. Rev. **C 53**, 752 (1996).
- [31] T. Yamada, Nucl. Phys. **A687**, 297c (2001).
- [32] M. Yosoi, H. Akimune, I. Daito, H. Ejiri, H. Fujimura, M. Fujiwara, T. Ishikawa, M. Itoh, T. Kawabata, M. Nakamura, T. Noro, E. Obayashi, H. Sakaguchi, H. Takeda, T. Taki, A. Tamii, H. Toyokawa, N. Tsukahara, M. Uchida, T. Yamada, and H.P. Yoshida, Phys. Lett. **B551**, 255 (2003).
- [33] T. Yamada, M. Yosoi, , and H. Toyokawa, Nucl. Phys. **A738**, 323 (2004).
- [34] K. Kobayashi, H. Akimune, H. Ejiri, H. Fujimura, M. Fujiwara, K. Hara, K.Y. Hara, T. Ishikawa, M. Itoh, Y. Itow, T. Kawabata, M. Nakamura, H. Sakaguchi, Y. Sakemi, M. Shiozawa, H. Takeda, Y. Totsuka, H. Toyokawa, M. Uchida, T. Yamada, Y. Yasuda, H.P. Yoshida, M. Yosoi, and R.G.T. Zegers, arXiv:nucl-ex/0604006.
- [35] C. Mahaux, P.E. Bortignon, R.A. Broglia, and C.H. Dasso, Phys. Rep. **120**, 1 (1985).
- [36] N. Frazier, B. A. Brown, and V. Zelevinsky, Phys. Rev. **C54**, 1665 (1996).
- [37] A. J. Sargeant, M. S. Hussein, M. P. Pato, and M. Ueda, Phys. Rev. **C61**, 011302(R) (1999).
- [38] A.H. Wapstra and N. B. Gove, Nucl. Data Tables **9**, 265 (1971).
- [39] C. Bennhold and A. Ramos, Phys. Rev. **C45**, 3017 (1992).
- [40] E. Bauer, A. P. Galeão, M. S. Hussein, and F. Krmpotić, arXiv:0808.0531.